

Verification of simulated snow cover in an Arctic basin using satellite-derived snow-cover maps

O. C. TURPIN,¹ R. G. CAVES,² R. I. FERGUSON,¹ B. JOHANSSON³

¹*Sheffield Centre for Earth Observation Science, Department of Geography, University of Sheffield, Sheffield S10 2TN, England*

²*Sheffield Centre for Earth Observation Science, School of Mathematics and Statistics, University of Sheffield, Sheffield S3 7RH, England*

³*Research and Development Department, Swedish Meteorological and Hydrological Institute, S-601 76 Norrköping, Sweden*

ABSTRACT. Time series of Earth observation (EO) data (Landsat Thematic Mapper (TM), U.S. National Oceanic and Atmospheric Administration Advanced Very High Resolution Radiometer (NOAA AVHRR) and European Remote-sensing Satellite synthetic-aperture radar (ERS SAR)) were obtained for a 2250 km² mountainous basin in northern Sweden to validate snow-cover area (SCA) estimates produced by a conceptual model (HBV) during three melt seasons. SCA depletion curves derived for each image type, and coincident images, reveal that the SCA estimate varies with the sensor. Discrepancies between TM and AVHRR appear to be an effect of spatial resolution. However, differences between TM and SAR are not simply related. Since more AVHRR than TM data were available, a TM-equivalent SCA was derived from AVHRR by relating TM SCA to AVHRR channel 1 reflectance. The TM-equivalent SCA was used to test SCA simulated by HBV for the 1992 melt season. Although the modelled and TM-equivalent SCA were in reasonable agreement, the modelled SCA declined faster than the TM-equivalent SCA. Partial recalibration of model parameters controlling snowpack accumulation improved the match between the modelled and EO-derived SCA decline. The recalibrated parameters were verified using SCA maps generated for the 1996 and 1998 melt seasons. The adjusted parameter sets had little effect on the Nash–Sutcliffe R^2 runoff fit but improved the volume fit in all three years.

INTRODUCTION

The timing and volume of runoff from predominantly snow-covered mountainous basins is determined by the interplay between snow accumulation and seasonal heat energy input to the snowpack. Conceptual snowmelt-runoff models must either assume a mean snow-water equivalent (SWE) and distribution at the beginning of the modelled melt season or accumulate snowfall throughout the preceding winter (Turpin and others, 1999). The latter approach is taken by many general-purpose conceptual hydrological models with a snow routine.

Runoff simulations generated by such models may be imperfect not because of any problem with the snowmelt routine or its parameter values, but because of errors in the simulated snowpack, for example, through uncertainties in the precipitation gradient or the threshold temperature below which rain turns to snow (Ferguson, 1999). Validation of snowpack properties or related parameters can therefore reveal inadequacies in the model structure or parameterization (Bergström, 1991). Spatial and temporal measurements of SWE are most suitable for this task since general-purpose models with a snow routine track SWE change due to snow accumulation and melt. Ground surveys of SWE are long-established but time-consuming. Hence, the data produced are rarely frequent, detailed or extensive enough for model validation. Passive-microwave satellite sensors are able to measure SWE, but the coarse spatial resolution restricts their use to homogeneous flat areas (Rango, 1996). SWE can be mapped moderately well in open areas using airborne gamma radiation (e.g. Bergström and Brandt, 1985), but the signal

is hard to distinguish from biomass attenuation in forests (Carroll and Carroll, 1989), and the technique is impractical in mountainous basins since low-level overpasses are required to reduce atmospheric attenuation of the signal. While detailed observations of SWE are difficult to acquire, high-resolution snow-cover area (SCA) measurements can be obtained from remote-sensing data. For example, Brandt (1991) used airborne radar to update the modelled snowpack, while Häggström (1994) and Turpin and others (1997) compared simulated snow cover with Advanced Very High Resolution Radiometer (AVHRR) and Thematic Mapper (TM) data, respectively.

Snow maps from three satellite sensors (Landsat TM, U.S. National Oceanic and Atmospheric Administration (NOAA) AVHRR and European Remote-sensing Satellite synthetic-aperture radar (ERS SAR)) were obtained over three melt seasons for a basin in Arctic Sweden. Differences in SCA derived from the three sensor types are analyzed and the implications for validation of modelled SCA are highlighted. The comparison led to a reclassification of the NOAA AVHRR imagery to give snow-cover proportion per pixel. These data were used to test the SCA predictions generated by the Swedish HBV model (Lindström and others, 1997) with different parameter sets for one melt season, and then verify SCA predictions for two subsequent melt seasons.

TJAKTJAJAURE BASIN

The Tjaktjajure basin drains part of the Sarek mountains in northern Sweden. It is approximately 2250 km² in area, ranges in altitude from 450 to 2044 m a.s.l. (mean 933 m)

Table 1. Physiographic characteristics of the four Tjaktjajaure sub-basins

Sub-basin	Area km ²	Elevation range m
Laitaure	104	450–1300
Litnok	659	500–2044
Sitojaure	689	600–1700
Tjaktjajaure	797	450–1200

and is located between 67° and 67°30' N. The area is characterized by compact massifs surrounding a broad open valley, with steep and narrow side valleys. The basin supports some forest below 800 m (18% of the basin) but is devoid of soil cover above 1000–1200 m, consisting only of boulders and bare rock (Carlsson, 1997). Lakes constitute 6% of the basin area, while higher elevations are glacierized (6% of the basin). There are no meteorological stations within the basin, but interpolation of data from surrounding stations indicates a strong east–west precipitation gradient: the mean annual precipitation varies from 700 mm in the east to almost 2000 mm in the west. Annual evapotranspiration is estimated at 200 mm, and the mean annual temperature is around -3°C. The large Tjaktjajaure outlet reservoir is heavily regulated by a hydropower plant. For hydrological simulations and Earth observation (EO) data analysis the Tjaktjajaure basin was divided into four sub-basins (Table 1).

SNOW-COVER DATA

Time series of EO data (Landsat TM, NOAA AVHRR and ERS SAR) for three melt seasons (1992, 1996 and 1998) were geocoded and classified into snow and non-snow using physically based binary decision methods. In all cases sub-pixel geocoding accuracy was achieved.

Snow cover is detected in Landsat TM images using the ratio of planetary reflectance in band 3 (red) to band 5 (shortwave infrared). Rott and Markl (1989) classified areas with a ratio of >2.7 as snow. Subjective assessment of the Tjaktjajaure snow maps indicated that a threshold value of 3.0 was more appropriate. This rule misclassified some areas (e.g. water) with a low reflectance in band 3 but an even lower reflectance in band 5. To prevent this, snow is detected only when band 3 reflectance is >0.10.

AVHRR snow maps were generated from midday images, pre-calibrated to planetary reflectance (channels 1 and 2) or brightness temperature (channels 3–5). Images were classified into cloud, vegetation, snow and other using the hierarchical scheme of Voigt and others (1999). Snow is classified when band 1 reflectance is ≥0.25 (except where cirrus cloud is classified, when the threshold is raised to 0.30) in areas that have not already been classified as cloud or vegetation.

The wet-snow mapping method of Nagler and others (1998) was used to classify wet snow in ERS SAR images. There are two steps. First, a ratio image is generated from the image thought to contain wet snow and a reference image which is known to contain no or dry snow. Second, backscatter ratios less than or equal to a predefined threshold are classified as wet snow. After a sensitivity analysis was conducted, a threshold of -3 dB was chosen for all SAR images. The same threshold was successfully used in alpine basins to detect wet snow from C-band SAR imagery. The method can be applied in areas of layover or radar shadow, and performs poorly at local incidence angles of <17° or >78° (Nagler, 1996). Within discrete elevation/aspect classes these areas of missing coverage were inferred to be wet snow if detected wet snow already formed most of the non-missing coverage areas. Dry snow was inferred uphill of large areas of wet snow (>1 km²), above the mean elevation of wet snow and uphill from wet snow, or 200 m above the mean elevation of wet snow.

Caves and others (2000) give a fuller description of the geocoding and classification methods used. SCA classification from optical sensors is hampered by cloud. Snow in these regions was interpolated from unaffected areas using topographic variables. Sub-basin snow maps were not generated for imagery with 50% or more cloud.

Throughout a melt season the time series of snow-cover maps show a progressive reduction in SCA. However, there are considerable discrepancies between SCA values derived from the three sensors (Fig. 1). AVHRR snow maps indicate a larger SCA than TM snow maps, which are snowier than SAR snow maps. A detailed comparison of images that were coincident or near-coincident (within a couple of days when little snowmelt was known to have occurred) was conducted to investigate the reasons for these differences (Caves and others, 1999). This indicated that agreement between TM and AVHRR is best on flat and gently sloping areas, such as glaciers. In narrow valleys and on steep slopes TM detects patchy snow, whereas AVHRR snow maps indicate continuous snow (although where snow is very patchy it is shown

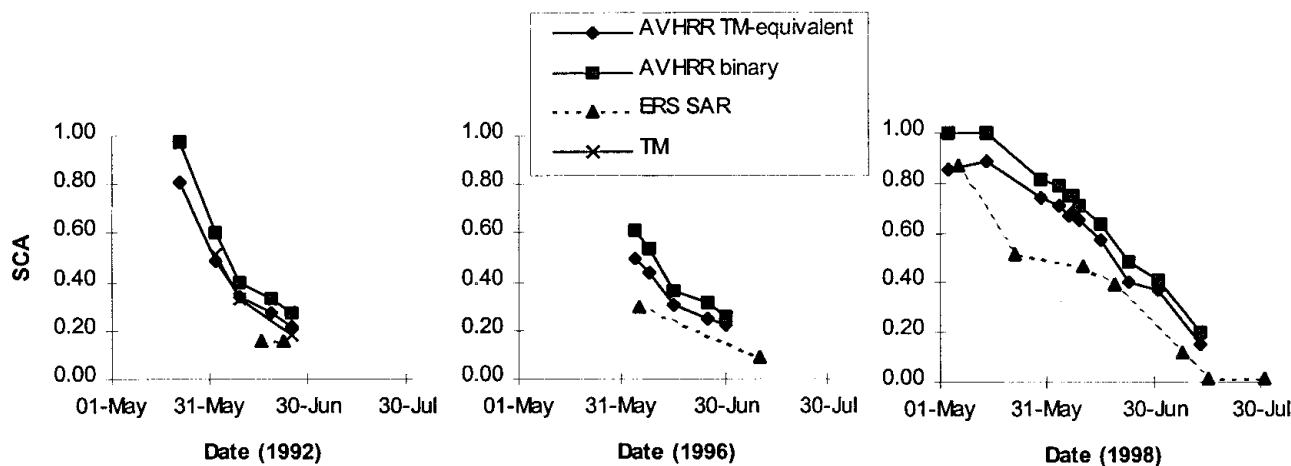


Fig. 1. SCA depletion determined from EO data (NOAA AVHRR, Landsat TM and ERS SAR) for the Tjaktjajaure basin.

only by the TM snow maps). The SAR classification fails to detect patchy snow at lower elevations but shows more snow than TM at higher elevations, partly due to erroneous dry-snow inference. Although AVHRR snow maps reveal more snow than TM, estimates from both sensors vary in a similar manner with elevation. A different pattern is shown on the SAR snow maps. In these the SCA maximum occurs at a higher elevation, and SCA declines more rapidly as the basin is descended than for either AVHRR or TM.

It is clear that SCA estimates from different sensors cannot be assumed to be equivalent for calibration or verification of modelled SCA. In the absence of field data, TM snow maps were assumed to be nearest to truth since TM has a finer spatial resolution than AVHRR, and production of SAR snow maps requires spatial averaging and dry-snow inference. Since the differences between AVHRR and TM snow maps appear to be a systematic effect of spatial resolution a method was developed to estimate TM-equivalent SCA from AVHRR.

Based on three dates in 1992 for which there are coincident AVHRR and TM images, the snow-covered proportion of each AVHRR pixel, P_s , as determined from the coincident TM snow map, was related to AVHRR channel 1 reflectance, R_1 (Caves and others, 1999). Each date shows a strong positive linear relationship (correlation coefficient >0.85). The average linear function

$$P_s = \begin{cases} 0 & \text{if } R_1 < 0.08 \\ 1.63R_1 - 0.13 & \text{if } 0.08 \leq R_1 \leq 0.69 \\ 1 & \text{if } R_1 > 0.69 \end{cases} \quad (1)$$

based on all three dates was used to relate cloud-free AVHRR channel 1 reflectance, R_1 , to TM-equivalent snow cover. As for the binary snow classification, snow in cloud-covered areas was interpolated from cloud-free areas using topographic variables.

As expected, the AVHRR TM-equivalent SCA estimates for the Tjaktjajaure basin were similar to the TM-estimated SCA. There was slightly more variation for the sub-basins than for the Tjaktjajaure basin as a whole. The AVHRR TM-equivalent snow map on 2 June showed a little less snow than the TM snow map in three sub-basins (maximum difference 6% in Sitojaure), while the AVHRR TM-equivalent snow map on 25 June showed slightly more snow than the TM snow map in all sub-basins (maximum difference 4% in Sitojaure and Laitaure). The AVHRR TM-equivalent and TM snow maps for 9 June were very similar.

Dissimilarities between TM and SAR are not so simply related as differences between TM and AVHRR. Thus, it has not yet been possible to devise a method to estimate TM-equivalent SCA from SAR.

CONCEPTUAL SNOWPACK MODELLING WITHIN HBV

HBV is a general-purpose hydrological model that simulates snow accumulation and melt, soil-moisture fluctuations, ground-water flow and runoff generation from daily values of temperature and precipitation (Bergström, 1992). The modelled basin can be disaggregated into sub-basins to allow for time lags in runoff from different parts of a large basin or for regional gradients in precipitation. The snow and soil components can be further subdivided into elevation zones and four land-cover classes: forest, glacier, lake and open (short vegetation, bare rock, etc.). Only the snow component, described below, is relevant to this study. SMHI (1996) and

Lindström and others (1997) provide a complete description of the most recent version of the model (HBV-96).

Input data may be taken from one or more meteorological stations. In the latter case, stations are weighted to form a composite station. Precipitation may also be rescaled by a general correction factor and under-catch correction factors for rain, snowfall in forest and snowfall in other areas. Precipitation recorded at a real or composite station is extrapolated to each elevation zone using a linear gradient of the form:

$$P_z = P_{\text{stat}} \left[1 + \frac{\text{pcalt}(h_z - h_{\text{stat}})}{100} \right], \quad (2)$$

where P_z is the precipitation (mm) extrapolated to zone z , P_{stat} is the precipitation (mm) measured at the station, pcalt is the precipitation gradient (per 100 m) and h_z and h_{stat} are the altitude (both m a.s.l.) of the zone and the station, respectively. An upper limit, pcaltl (m a.s.l.), can be set for pcalt , above which precipitation may increase at a different rate, often zero, and a separate gradient can be used for glacier zones. In this case P_{stat} (mm) in Equation (2) is replaced by the precipitation at pcaltl , P_{pcaltl} (mm), and h_{stat} is replaced by pcaltl . P_{pcaltl} is computed as:

$$P_{\text{pcaltl}} = \frac{P_{\text{stat}}}{1 + \text{pcalt}(h_{\text{stat}} - \text{pcaltl})/100}. \quad (3)$$

Precipitation form is dependent on the elevation of the freezing level. As high-level temperature measurements are rarely available, HBV extrapolates temperature using a lapse rate. The occurrence of rain or snow is determined from the extrapolated air temperature using a threshold temperature or ramp change between two temperatures. The threshold is critical, as an incorrect assumption will lead to an erroneous snowpack size. The problem is particularly acute for models such as HBV that use daily precipitation and temperature, as neither the temperature during precipitation nor the time of precipitation is known.

Snowmelt is simulated using a degree-day melt coefficient when the air temperature in a zone is above a critical temperature. The melt coefficient can be different for forest zones. Snowmelt is retained in the snowpack until a water-holding capacity is exceeded. If air temperature drops below the critical temperature, snowmelt held within the snowpack is assumed to refreeze.

HBV allows for variable SWE within elevation zones (Lindström and others, 1997; Turpin and others, 1999) by separating SWE into a number of equal-area subzones whose SWE values form an arithmetic series centred on the zone mean (Fig. 2). The relative SWE increase between subzones is given by a distribution factor that may be different in forest and non-forest. SCA is implicitly tracked as the snow in each subzone and elevation zone melts out.

HBV SIMULATION OF THE TJAKTJAJAURE BASIN

The four sub-basins of the Tjaktjajaure basin were each further divided into 100 m elevation bands and land-cover classes, giving a total of 64 sub-areas ranging in area from 1 to 177 km² (average 35 km²). The only available input data were from four low-level meteorological stations outside the basin. Runoff from the basin was computed from reservoir-level data, outflow through the hydropower plant turbines and spill through its gates. The model was calibrated on 10 years' continuous daily runoff data (September 1976–August 1986) using an automatic optimization procedure

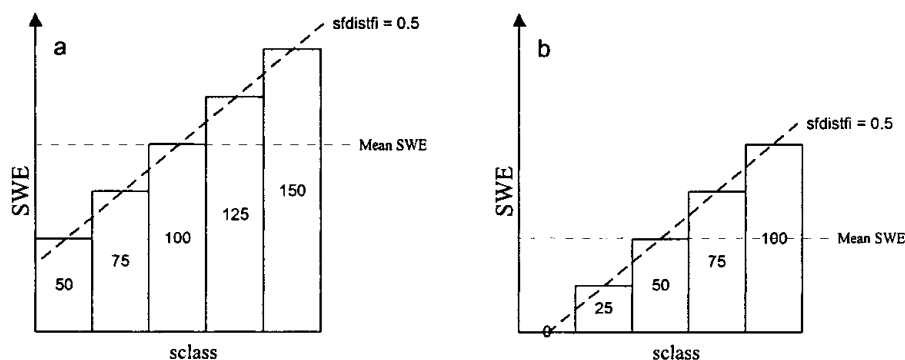


Fig. 2. Distribution of SWE within a zone with sclass = 5 and sfdistfi = 0.5. (a) Distribution of 100 units of SWE after snowfall. (b) Result of melting 50 units of SWE.

(Lindström, 1997), and validated on a further 10 years’ runoff data (September 1986–August 1996). It produced very good Nash–Sutcliffe R^2 fits for both the calibration and verification periods (0.87 and 0.84, respectively) with only slight volume underestimations (−0.8% and −1.3%, respectively). The Nash–Sutcliffe R^2 fits for each of the three years with EO data were also very good, although discharge was under-predicted in each year (Table 2).

SNOWPACK RECALIBRATION AND VERIFICATION USING EO DATA

Landsat TM data were initially used to verify HBV snowpack predictions during the 1992 melt season. The TM snow maps (Fig. 3) show that on 2 June the modelled SCA is too high, especially in the lower, predominantly forested, basins (Laitaure and Tjaktjajaure), but that simulated SCA declines too fast through June so that SCA is greatly under-predicted on 25 June in the upper, mostly open, basins (Litnok and Sitojaure). Between 2 and 25 June the default HBV parameter set simulates 56% of the Litnok and 38% of the Tjaktjajaure sub-basin area to become snow-free, while the TM snow maps indicate only 34% and 26% SCA depletion, respectively.

Since 1992 SCA simulations were poor, model parameters that affect snowpack accumulation and ablation were recalibrated with the aim of improving snowpack simulation while retaining good runoff simulations. Several parameters that affect snow cover are set at fixed values before HBV is calibrated. These include the meteorological-station weights used for estimation of areal precipitation and temperature, the precipitation gradient (pcalt) and its upper limit (pcaltl), the temperature lapse rate, the number of snow classes within

an elevation zone and the snowpack distribution within an elevation zone (sfdistfi).

For the purposes of calibration and verification of the model against runoff, precipitation weights were set subjectively, based on the distance of each meteorological station from the centre of the basin. To improve snowpack simulation in each of the sub-basins, the precipitation weightings were recalculated using Thiessen polygons to account for the proximity of each meteorological gauge to each sub-basin. This had little impact on the simulated SCA or the Nash–Sutcliffe R^2 runoff fit but increased under-prediction of runoff for the 1992 melt season. The revised meteorological weightings were retained since theoretically they provide a better areal estimation of the precipitation received by the Tjaktjajaure basin.

For HBV simulations, it is usually assumed that precipitation does not increase above the tree line (approximately 800 m in the Tjaktjajaure basin). Hence, the default settings (used for model calibration) were pcalt = 0.1 per 100 m and pcaltl = 800 m (also termed run 1). By modification of pcalt and pcaltl the distribution of snow with elevation can be altered (Fig. 4). Since the nature and size of the snowpack in a basin may vary annually, modifications to snowpack parameters that are advantageous in one melt season may be detrimental in another. Ideally time series of TM snow maps would be available for other melt seasons to enable the effect of alterations to snowpack parameters to be verified. Instead, TM-equivalent snow maps generated from AVHRR imagery were used to calibrate and verify the effect of snowpack parameter changes on HBV SCA predictions.

Table 2. Discharge fits generated by model runs 1–4 for the Tjaktjajaure basin in 1992, 1996 and 1998 (1 September–31 August in each case). Fits calculated using Nash–Sutcliffe R^2 and relative volume deviation (D_v). Volume under-predictions shown as negative

	1992		1996		1998	
	R^2	D_v	R^2	D_v	R^2	D_v
		%		%		%
Default (run 1)	0.90	−1.8	0.89	−11.1	0.87	−6.8
Run 2	0.91	−14.8	0.86	−20.7	0.83	−19.8
Run 3	0.91	−0.7	0.91	−8.3	0.88	−6.0
Run 4	0.90	−1.4	0.91	−8.5	0.87	−6.2

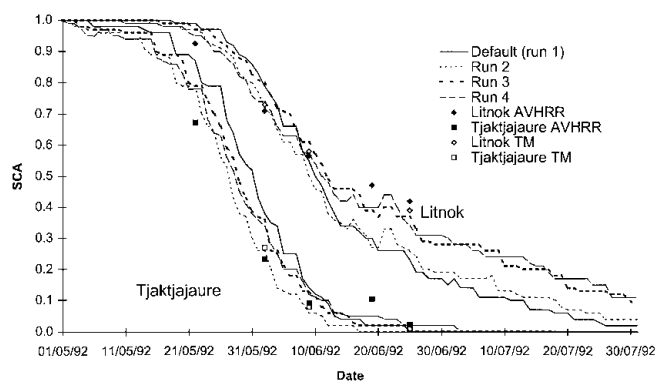


Fig. 3. HBV SCA simulation for the Litnok and Tjaktjajaure sub-basins generated by runs 1–4 for the 1992 melt season with TM and AVHRR TM-equivalent SCA (<50% clouds) for comparison. To improve clarity only two basins are shown. Dates are dd/mm/yy.

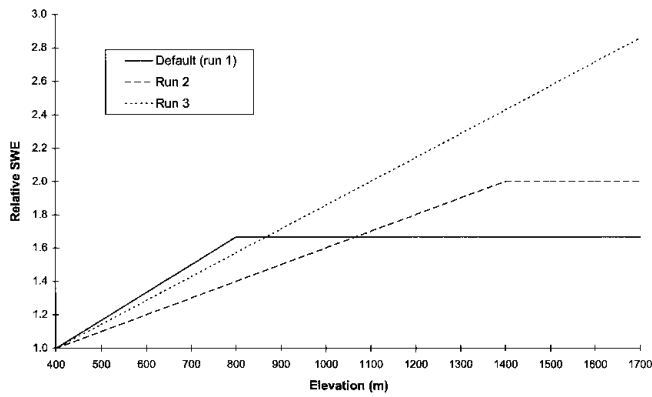


Fig. 4. Relative SWE (compared to unit snowfall at an average station elevation of 400 m) for three parameter combinations: default (run 1): $pcalt = 0.1$ per 100 m, $pcaltl = 800$ m; run 2: $pcalt = 0.05$, $pcaltl = 1400$; and run 3: $pcalt = 0.05$, $pcaltl = 1700$.

With $pcalt = 0.05$ per 100 m and $pcaltl = 1400$ m (run 2) the TM snow maps show that SCA was predicted extremely well on 2 June in the Litnok and Sitojaure sub-basins, and reasonably well on all three TM dates (2, 9 and 25 June) in the Tjaktjajaure and Laitaure sub-basins. However, SCA depletion was still too fast in the upper two basins, resulting in under-prediction of SCA on 9 and 25 June (Fig. 3). With $pcalt = 0.05$ per 100 m and $pcaltl = 1700$ m (run 3) SCA was over-predicted on 2 and 9 June in all four sub-basins but simulated reasonably well on 25 June.

Runs 2 and 3 over-predict the AVHRR TM-equivalent SCA on 22 May and under-predict the AVHRR TM-equivalent SCA on 19 June in each of the four sub-basins. Increasing $sfdistfi$ increases the variability of SWE within an elevation-zone-land-cover class. Hence, SCA reduces slightly more quickly at the beginning of the melt season as shallower SWE subzones melt out, but remains higher for longer towards the end of the melt season as deeper SWE subzones take longer to melt out. With $pcalt = 0.05$ per 100 m, $pcaltl = 1700$ m (the values used for run 3) and $sfdistfi = 0.7$ (termed run 4) the simulated SCA reduces more rapidly at the beginning of the melt season than for any of the other runs. Thus the simulation of the TM-equivalent SCA on 22 May is improved. Subsequently SCA reduces more gradually, producing good SCA predictions on 2 and 9 June in the upper two basins. Since SCA remains

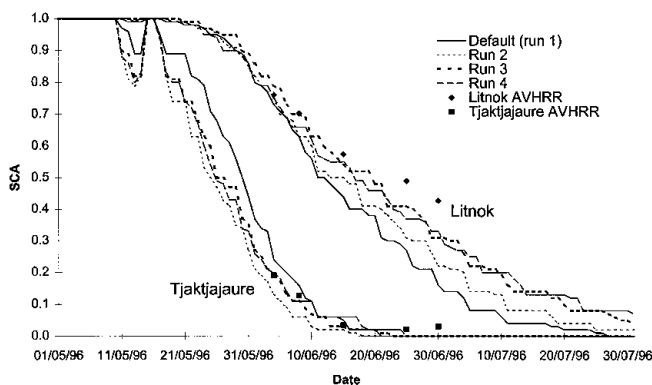


Fig. 5. HBV SCA simulation for the Litnok and Tjaktjajaure sub-basins generated by runs 1–4 for the 1996 melt season with AVHRR TM-equivalent SCA (<50% clouds) for comparison. Dates are dd/mm/yy.

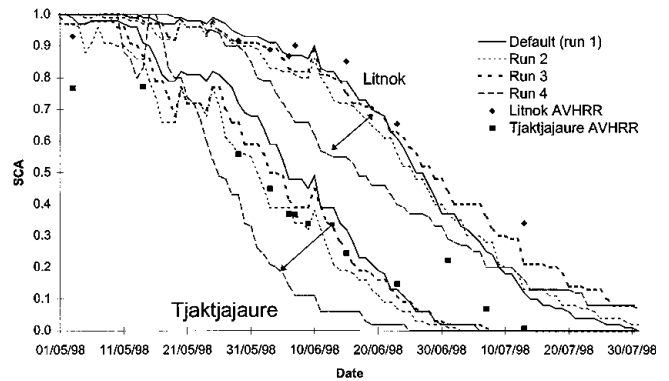


Fig. 6. HBV SCA simulation for the Litnok and Tjaktjajaure sub-basins generated by runs 1–4 for the 1998 melt season with AVHRR TM-equivalent SCA (<50% clouds) for comparison. Dates are dd/mm/yy.

high towards the end of the melt season, SCA simulation on 19 and 25 June was also better. However, run 2 simulated SCA better on 2 and 9 June in the lower two sub-basins.

The recalibrated parameter settings were verified using TM-equivalent SCA for 1996 and 1998. The five TM-equivalent snow maps for 1996 (Fig. 5) show SCA depletion curves very similar to those in the 1992 snow maps for the Sitojaure, Laitaure and Tjaktjajaure sub-basins. The Litnok sub-basin had a little more snow than in 1992. Hence, SCA reduction occurred slightly later. SCA in the Sitojaure and Litnok sub-basins is simulated well on 4 and 8 June by all runs. Runs 3 and 4 maintain good SCA estimations on 15 June, although SCA predicted by runs 1 and 2 declines too rapidly throughout June, under-predicting the TM-equivalent SCA. Runs 3 and 4 also under-predict the TM-equivalent SCA on 25 and 30 June, but by a smaller amount. Over the whole melt season, run 4 is the best simulator of SCA in the upper basins as its SCA decline is most gradual. The SCA simulations produced by all runs for the lower Laitaure and Tjaktjajaure sub-basins were very good. Very little TM-equivalent SCA decline occurred which coincided with the tail end of the model-predicted SCA depletion.

Model simulations and EO-derived snow maps show that SCA was greater in all sub-basins throughout the 1998 melt season (Fig. 6) than in 1992 or 1996. Run 3 generated the best SCA predictions in all sub-basins. In the Litnok sub-basin there was a tendency to under-predict the TM-equivalent SCA towards the end of the melt season. Run 4 produced very poor SCA predictions in all four sub-basins. Apart from early and mid-May it under-predicted the TM-equivalent SCA throughout the melt season in all sub-basins. All parameter sets overestimated SCA at the beginning of May in all four sub-basins.

Run 2 had a slightly negative impact on the R^2 runoff fit in 1996 and 1998. Runs 3 and 4 either had no effect or caused a slight improvement in the R^2 runoff fit in all three years. Furthermore, they both gave better volume fits than the default parameter settings (Table 2).

DISCUSSION AND CONCLUSIONS

It has been proposed that a conceptual hydrological model may have a number of parameter sets that are equally proficient in terms of runoff prediction (Beven and Binley, 1992). In this study it has been possible to improve the simulation

Table 3. Summary of SCA fits for the Tjaktjajaure basin

	No. of observations	Default (run 1)	Run 2	Run 3	Run 4
1 Laitaure sub-basin	22	0.82	0.70	0.84	0.66
Litnok sub-basin	19	0.06	0.30	0.77	0.40
Sitojaure sub-basin	18	0.68	0.71	0.81	0.58
Tjaktjajaure sub-basin	22	0.74	0.77	0.87	0.73
Tjaktjajaure (whole basin)	21	0.64	0.63	0.83	0.61
2 1992†	20	0.67	0.78	0.83	0.89
1996†	20	0.33	0.35	0.81	0.83
1998†	41	0.73	0.72	0.84	0.07
3 All†	81	0.58	0.62	0.82	0.59

Notes: 1. Mean of three melt seasons' Nash–Sutcliffe R^2 values; 2. Mean of four sub-basins' Nash–Sutcliffe R^2 values; 3. Mean of 12 Nash–Sutcliffe R^2 values (three melt seasons and four sub-basins).

† Does not include the whole basin.

of the snowpack via small modifications to the parameters affecting snow accumulation without detrimental effects on the runoff fit. Indeed runs 3 and 4 resulted in improved runoff fits, in terms of both Nash–Sutcliffe R^2 and volume error (Table 2), relative to the default parameter settings.

Careful adjustment of the precipitation weightings and a selection of the snow accumulation and distribution parameters led to progressive improvement in the simulated SCA for 1992 (Table 3). Run 3 maintained good SCA fits for the 1996 and 1998 melt seasons. However, although run 4 performed well during 1996 it failed to adequately simulate SCA depletion in 1998. Similarly the SCA fit for run 2 was poor in 1996 despite reasonable fits in 1992 and 1998. Overall, the parameter sets simulated the lower basins marginally better than the upper basins, with run 3 achieving the best R^2 fits. The SCA R^2 fit generated by the default parameter set (run 1) for the Litnok sub-basin was substantially poorer than the fit for any other sub-basin. Although runs 2–4 simulate SCA depletion in the other three sub-basins better than in Litnok, the best SCA R^2 improvement is generated for Litnok. Run 4 generates poorer SCA fits for each sub-basin than the default parameter set. This is due to its weaker performance in 1998, as fits in 1992 and 1996 are better than the default parameter set.

So far in this paper it has been assumed that discrepancies between modelled SCA and the AVHRR-generated TM-equivalent SCA are due to inadequacies in model simulation of the snowpack. However, it is also probable that the AVHRR TM-equivalent SCA is not a perfect representation of the true SCA. Even though TM has a better spatial resolution than AVHRR, snow maps generated from TM are likely to be a misrepresentation of the true SCA. Furthermore, the empirical function used to relate AVHRR channel 1 reflectance to TM snow-covered proportion is based on three dates with similar solar illumination angles, TM-classified snow cover in mainly non-forested parts of the basin, and virtually no cloud. It may not hold so well earlier in the melt season when larger areas below the tree line are still snow-covered, solar incidence angles are lower and the area of shadow is greater. Snow interpolation from cloud-free to cloud-covered regions of AVHRR imagery is likely to further increase the error in an SCA estimate. If coincident AVHRR–TM pairs were available early in the melt season, it might be possible to derive separate relation-

ships for forest and non-forest areas and to include a correction for shading.

ACKNOWLEDGEMENTS

This work was funded by the European Union, DG-XII, contract ENV4-CT96-0364 (Hydrology of Alpine and High Latitude Basins).

REFERENCES

- Bergström, S. 1991. Principles and confidence in hydrological modelling. *Nord. Hydrol.*, **22**, 123–136.
- Bergström, S. 1992. *The HBV model — its structure and applications*. Norrköping, Sweden, Sveriges Meteorologiska och Hydrologiska Institut. (SMHI Report RH 4.)
- Bergström, S. and M. Brandt. 1985. Measurement of areal water equivalent of snow by natural gamma radiation — experiences from northern Sweden. *Hydrol. Sci. J.*, **30**, 465–477.
- Beven, K. and A. Binley. 1992. The future of distributed models: model calibration and uncertainty prediction. *Hydrol. Processes*, **6**, 279–298.
- Brandt, M. 1991. *Snösmätning med georadar och snötaxeringar i övre Luleälven*. Norrköping, Sweden, Sveriges Meteorologiska och Hydrologiska Institut. (SMHI — Hydrology Report 33.)
- Carlsson, U. 1997. The Swedish mountains. *Alpine Journal* 1997, 144–147.
- Carroll, S. S. and T. R. Carroll. 1989. Effect of forest biomass on airborne snow water equivalent estimates obtained by measuring terrestrial gamma radiation. *Remote Sensing Environ.*, **27**(3), 313–319.
- Caves, R., O. C. Turpin, C. Clark, R. Ferguson and S. Quegan. 1999. Comparison of snow covered area derived from different satellite sensors: implications for hydrological modelling. In *RSS '99, Earth Observation — from Data to Information, 8–10 September 1999, University of Wales at Cardiff*. Cardiff, University of Wales. Remote Sensing Society, 545–552.
- Caves, R. G., O. C. Turpin, C. D. Clark, R. I. Ferguson, S. Quegan and B. Johansson. 2000. The use of Earth observation for monitoring snowmelt runoff from non-alpine basins. In *19th EARSel Symposium, Remote Sensing in the 21st century: Economic and Environmental Applications, 31 May–2 June 1999, Valladolid, Spain. Proceedings*. Rotterdam, A.A. Balkema, 183–190.
- Ferguson, R. I. 1999. Snowmelt runoff models. *Prog. Phys. Geogr.*, **23**(2), 205–227.
- Hägström, M. 1994. *Snow mapping in Swedish mountains using NOAA satellite data*. Norrköping, Sweden, Sveriges Meteorologiska och Hydrologiska Institut. (SMHI Report RH 57.)
- Lindström, G. 1997. A simple automatic calibration routine for the HBV model. *Nord. Hydrol.*, **28**(3), 153–168.
- Lindström, G., B. Johansson, M. Persson, M. Gardelin and S. Bergström. 1997. Development and test of the distributed HBV-96 hydrological model. *J. Hydrol.*, **201**, 272–288.
- Nagler, T. 1996. Methods and analysis of synthetic aperture radar data from ERS-1 and X-SAR for snow and glacier applications. (Ph.D. thesis, University of Innsbruck.)
- Nagler, T., H. Rott and G. Glendinning. 1998. SAR-based snow cover retrievals for runoff modelling. In *2nd International Workshop on Retrieval of Bio- and Geophysical Parameters from SAR Data for Land Applications, 21–23 October 1998, Noordwijk. Proceedings*. Noordwijk, Netherlands, European Space Agency. ESTEC, 511–517. (ESA SP-441.)
- Rango, A. 1996. Spaceborne remote sensing for snow hydrology applications. *Hydrol. Sci. J.*, **41**(4), 477–494.
- Rott, H. and G. Markl. 1989. Improved snow and glacier monitoring by the Landsat thematic mapper. In *Proceedings of a Workshop on "Earthnet Pilot Project on Landsat Thematic Mapper Applications", held at Frascati, Italy in December 1987*. Noordwijk, Netherlands, European Space Agency, 3–12. (ESA SP-1102.)
- Sveriges Meteorologiska och Hydrologiska Institut (SMHI). 1996. *IHM: integrated hydrological modelling system manual: version 4.0*. Norrköping, Sweden, Sveriges Meteorologiska och Hydrologiska Institut.
- Turpin, O. C., R. I. Ferguson and C. D. Clark. 1997. Remote sensing of snowline rise as an aid to testing and calibrating a glacier runoff model. *Phys. Chem. Earth*, **22**(3–4), 279–283.
- Turpin, O., R. Ferguson and B. Johansson. 1999. Use of remote sensing to test and update simulated snow cover in hydrological models. *Hydrol. Processes*, **13**(12–13), 2067–2077.
- Voigt, S., M. Koch and M. F. Baumgartner. 1999. A multichannel threshold technique for NOAA-AVHRR data to monitor the extent of snow cover in the Swiss Alps. *International Association of Hydrological Sciences Publication* 256 (Symposium at Birmingham 1998 — *Interactions between the Cryosphere, Climate and Greenhouse Gases*), 35–43.